# Estimates of the magnitude of topographical effects on surface heat flow from finite element modelling

Gordon Webb[1]* and Ben Harrison[2]
[1] Northern Territory Geological Survey, PO Box 8760, Alice Springs NT 0871, Australia
[2] School of Earth Sciences, The University of Melbourne, Victoria 3010, Australia
* Corresponding author: gordon.webb@nt.gov.au

## Introduction

Surface heat flow calculations are employed by geothermal exploration companies to estimate the geothermal gradient down to depths of 3 km to 6 km. Surface heat flow is typically calculated from coincident thermal conductivity data or estimates, and temperatures obtained by drilling a slim-line hole down to depths of 300 m to 1000 m. At such shallow depths the effect of a variable surface topography needs to be considered when performing temperature extrapolations to greater depth. This is because, for a given crustal volume with an undulating surface, heat will tend to flow towards topographic lows and away from topographic highs as it migrates from the base to the ground surface. A linear approximation method was developed by Lees (1910) to correct for topography under idealised geometric mountain ranges.

This study presents results from a series of finite element method (FEM) models that predict the magnitude of variation of surface heat flow at the surface of a homogenous two-dimensional slice of crust with a uniformly curved surface. The results from this simple geometry are then compared to irregular topographic surfaces derived from real world examples.

The main advantage of using the FEM method, described in this study, - rather than the method described by Lees (1910) - is that any regular or irregular surface topography may be used.

Keywords: surface heat flow, temperature, numerical modelling, topography.

## Model Parameters

A series of two-dimensional model geometries were constructed with a flat base and sides and a sinusoidal top edge representing the topographic surface (Figure 1). The models were all 10 km deep (measured from the midway point of the surface curvature to the base) to minimise near-field effects in fixed boundary conditions. The surface topography has a sinusoidal form with a wavelength denoted by λ and maximum elevation difference denoted Δh.

The width of the models was scaled with respect to the x-axis to generate different values for the ratio Δh/λ. Fifteen model geometries were constructed with values of Δh/λ varying between 0.01 (representing subdued, long wavelength topography) and 0.9 (representing steep, short wavelength topography). Δh had a constant value of 412 m for each of the models. The lower Δh/λ values might represent the gently undulating terrains encountered in areas such as the Darling Ranges near Perth, while Δh/λ values of about 0.07 might represent areas of moderate topographic expression, such as the Flinders Ranges and Mt Lofty Ranges in South Australia.

The model volume was defined as "non-radiogenic granite" with an isotropic thermal conductivity ($k$) of 3.2 $W.m^{-1}.K^{-1}$, a heat capacity ($C$) of 8500 $J.kg^{-1}.K^{-1}$ and a density ($\rho$) of 2600 $kg.m^{-3}$.

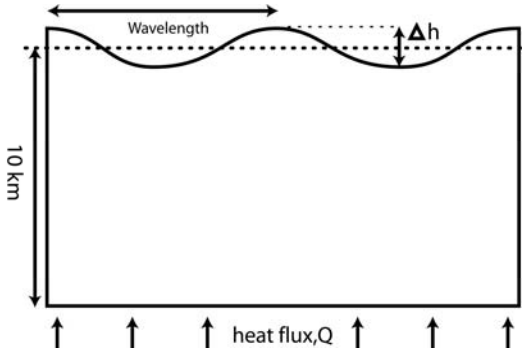


Figure 1: Diagram showing the generic geometry of the models.

A constant temperature of 20 degrees Celsius was maintained at the top surface of the models. The sides of the model were defined to be symmetrical and reflective to remove edge effects.

A uniform heat flux ($Q$) was applied to the bottom surface of each model. A basal heat flux of 60 $mW.m^{-2}$ was applied to each of the 15 models. Ten additional models were run with a basal heat flux of 80 $mW.m^{-2}$ for comparison. The models were meshed with a uniform Lagrange linear mesh with greater than 10,000 nodes per model space. The models were solved iteratively using the time-varying relationship,

$$\rho C\frac{\partial T}{\partial t} - \nabla \cdot (k\nabla T) = Q,$$

until the model residuals approach zero and a steady-state solution was attained.

## Results

Figure 2 shows the percentage decrease or increase in the modelled surface heat flow with

respect to basal heat flux at the highest and lowest topographic points, respectively. For relatively short wavelength topography (Δh/λ > 0.2) the modelled surface heat flow differs from the basal heat flux by greater than 50%. The modelled surface heat flow is within 5% of the basal heat flux value for very long wavelength, subdued topography (Δh/λ < 0.02).

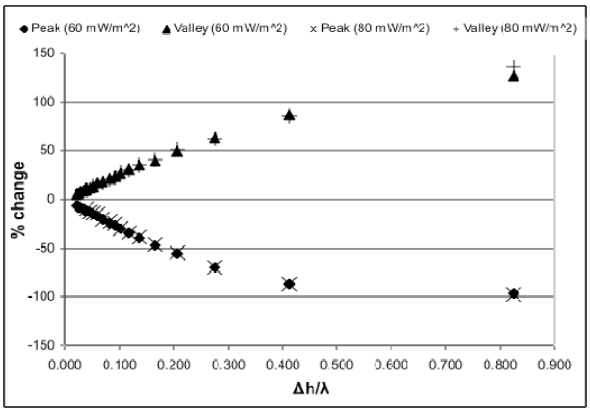


Figure 2: Plot of the percentage difference between the modelled surface heat flow with respect to the basal heat flux measured at the highest (peak; negative change) and lowest (valley; positive change) points on the surface topography.

Curves were generated below the highest and lowest topographic points that describe the vertical variation between the modelled surface heat flow and the basal heat flux (figure 3). Each pair of curves is a characteristic of the specific geometry of the model surface. An arbitrary point at which the curves have decayed to within 5% of the basal heat flux value can be usefully compared in each model to assess the depth at which the thermal perturbation is significantly diminished (figure 4). The depth of the thermal perturbation gradually increases with increasing wavelength (decreasing Δh/λ) until a maximum penetration is reached at a Δh/λ value of ~0.04 (figure 4).

## Discussion

The model solutions presented here represent an initial attempt to assess the magnitude of the variation of surface heat flow measurements with respect to regional heat flux due to the effect of topography using the finite element method. A number of other factors also affect surface heat flow measurement including (but not limited to) internal heat production, ground water flux, altitude/climate effects, and lateral thermal conductivity contrasts (Beardsmore and Cull, 2001 and references therein). The approach taken in this study deliberately ignores these other effects to specifically investigate the effect of topography in isolation.

These models predict that, for relatively short wavelength - high relief topography, surface heat flow measurements, will be significantly different from the regional, “deep” heat flux. For longer wavelength - low relief topography the observed difference will be less but may still be significant. These models also predict that the depth of thermal perturbation is related to the ratio of the relief height and the wavelength of surface topography and that this relationship is not linear.

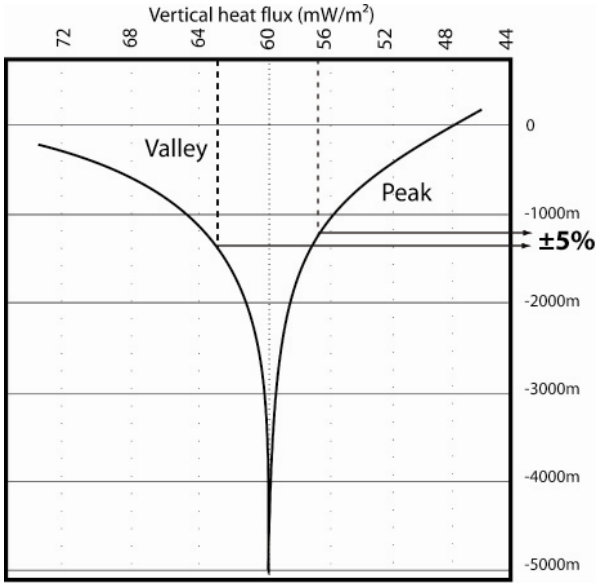


Figure 3: Profile of the modelled vertical heat flux below the peak (highest surface elevation) and the valley (lowest surface elevation) for model hft010 (Δh/λ = 0.082, λ = 5 km, Δh = 412 m). The decay of the thermal perturbation increases with depth until the basal heat flux value is reached. The 5% cut-off values used to generate figure 4 are shown.

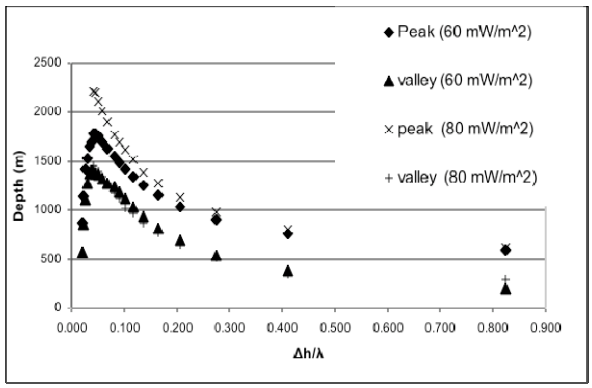


Figure 4: Plot of the depth at which the model heat flow is within 5% of the basal heat flux measured below the highest (peak) and lowest (valley) points on the surface topography. Note that the depth of perturbation attains a maximum value and then diminishes as a function of Δh/λ.

This study highlights a potentially significant source of uncertainty that must be factored in/corrected for when extrapolating heat flow data to depths of 3 km to 6 km. Furthermore, the results of this study suggest that the practice of estimating resource temperatures by calculating one-dimensional thermal models may only be valid for areas where surface topography is relatively subdued. In most other cases it is preferable to construct well parameterised two- and/or three dimensional thermal models.

## References

Beardsmore, G. R. & Cull, J. P. 2001 Crustal heat flow: a guide to measurement and modelling. Cambridge University Press.

Lees, C. H. (1910) On the Shapes of the Isogeotherms under Mountain Ranges in Radio-Active Districts. *Proceedings of the Royal Society of London*. Vol. 83, No. 563, pp. 339-346